VTL-PUB-35
(FEB. 1977)

PUB-77-127-E
E-0218

INCLUSIVE NEUTRAL PARTICLE PRODUCTION IN $\pi^- d$ INTERACTIONS AT 205 GeV*

S. Csorna, L. Dunn, H. J. Lubatti, H. Rudnicka**, K. Moriyasu, A. Zieminski***

Visual Techniques Laboratory, Department of Physics
University of Washington, Seattle, Washington 98195

H. Abramowicz, H. Bialkowska, J. Krolikowski, S. Otwinowski, A. Para, G. Sinapius†

University of Warsaw and Institute of Nuclear Research
Hoza 69, 00-681, Warsaw, Poland

J.H. Klems, W. Ko, R.L. Lander, D.E. Pellett, P.M. Yager

Department of Physics
University of California, Davis, California 95616

A. Eskreys, J. Figiel, D. Kisielewska, P. Malecki, P. Stopa, A. Zalewska

The Institute of Nuclear Physics and the Institute of Nuclear Physics and
Technology of the Academy of Mining and Metallurgy
Kawiory 26A, 30-055 Krakow, Poland

*Work supported in part by the National Science Foundation and E.R.D.A.

**Visitor from the Institute of Nuclear Physics and the Institute of Nuclear Physics and Technology of the Academy of Mining and Metallurgy, Krakow.

***Visitor from University of Warsaw and Institute of Nuclear Research, Warsaw.

†Supported by D.A.A.D. and P.A.N.

ABSTRACT

The inclusive production of neutral particles are studied in $\pi^- d$ interactions at 205 GeV. Topological distributions for the inclusive reactions $\pi^- d \to \gamma + x$, $\pi^- d \to K^o_S + x$, $\pi^- d \to \Lambda + x$ and the cross section for $\pi^- d \to \bar{\Lambda} + x$ are presented and compared with $\pi^- p$ and pp interactions at 100 and 205 GeV. The effects of double scattering are studied and $\pi^- n$ inclusive distributions are obtained and compared to results from $\pi^- p$ interactions (in hydrogen) at 205 GeV.

1. INTRODUCTION

We present results on inclusive neutral particle production in $\pi^- d$ interactions at 205 GeV. Data are derived from a 70,000 picture exposure of the FNAL 30-inch bubble chamber filled with liquid deuterium. Experimental details have been discussed in previous publications.[1,2] Scanning, measuring, and fitting procedures used to obtain the data in this paper are discussed in Section 2. The total and topological cross sections and momentum distributions for the inclusive reactions $\pi^- d \to \gamma + x$, $\pi^- d \to K^o_s + x$, $\pi^- d \to \Lambda + x$ and the cross section for the reaction $\pi^- d \to \bar{\Lambda} + x$ are presented in Section 3. In Section 4, we discuss double scattering effects in the above four reactions. In Section 5, we present $\pi^- n$ inclusive distributions and compare the results to a $\pi^- p$ experiment performed in a hydrogen-filled bubble chamber at the same energy.

2. DATA

The film was double scanned in three views on a life-sized projection for primary interactions of all topologies and associated neutral particles. Details concerning the beam, the scan, and the charged multiplicity distributions are presented in Ref. 1.

Slow proton tracks ($p < \sim 1.0$ GeV/c) and the tracks of V^o's and γ's pointing to the primary vertex were measured for all events. One-half of the sample of neutrals was processed with the TVGP-SQUAW chain of programs and the other with the CERN Hydra system. The fiducial volume was chosen such that each neutral had a potential decay path or materialization length of at least 10 cm. and a minimum charged decay track length of 10 cm. A study of the potential length distribution showed that for distances of the neutral vertex to the primary vertex greater than 2 cm. the detection

probability was uniform. V^o's and γ's were accepted only if the distance to the primary interaction was greater than 2 cm.; each event was weighed to correct for losses due to distances less than 2 cm.

Because of the small dimensions of the chamber, the detection efficiency is much larger for neutrals which are backwards in the center of mass.† For the detailed analysis, we shall restrict ourselves to the backward hemisphere and to $n_{CH} \geq 3$; however, we shall estimate the cross section for gammas produced in the forward hemisphere. The number of neutrals of each type (after all acceptance criteria were met) and the average weight based on detection efficiency and correction factors for scanning, measuring, and fitting losses are given in Table 1. The K/Λ ambiguities constitute 6% of the K^o_s events and 14% of the Λ events. We have verified that including these events does not significantly alter the physical distributions. The γ contamination in the K^o_s and Λ data samples is estimated to be less than 1.5% and 4%, respectively.

3. TOTAL AND TOPOLOGICAL CROSS SECTIONS FOR $\pi^- d$ INTERACTIONS

The number of fitted neutrals, the total cross sections, and the average number of neutrals per inelastic collision ($n_{CH} \geq 3$) are given in Table 1. We consider gammas produced both backwards and forwards in the center of mass but only K^o_s, Λ, and $\bar{\Lambda}$'s produced in the backward hemisphere. We note that the probability for producing a γ, K^o, or Λ in the backward hemisphere per inelastic collision is very nearly the same for $\pi^- d$, $\pi^- p$, and pp interactions at 205 GeV.

The dependence of neutral particle production on n_{CH} is given in Table 2. In Table 3 and Figs. 1a, b, c we present the dependence of the

---

†Forward γ's may be lost in the hadron shower, and fast, forward strange particles have a small probability of decay.

average number of neutral particles produced per inelastic interaction on the number of negative particles (n_-) produced: $\bar{N}_\gamma(n_-)$, $\bar{N}_{K^o_s}(n_-)$, $\bar{N}_\Lambda(n_-)$. The solid lines on Figs. 1b, c, and d are fits to the function $\alpha + \beta n_-$ from $n_- = 1$ to $n_- = 8$.

We note that $\bar{N}_\gamma$ is well represented by a linear dependence ($\alpha = 2.9 \pm 0.6$, $\beta = 1.1 \pm 0.2$) up to $n_- = 8$. Similar linear relationships in γ production have been observed in many experiments.[5)†] For $\bar{N}_{K^o_s}$ and $\bar{N}_\Lambda$ the data are consistent with little or no dependence on n_-: $\alpha = 0.043 \pm .005$ and $\beta = 0.013 \pm 0.002$ for $\bar{N}_{K^o_s}$; $\alpha = 0.028 \pm .005$ and $\beta = 0.006 \pm 0.002$ for $\bar{N}_\Lambda$. In π^-p interactions at 100 GeV[7)] and 205 GeV[3)] essentially flat distributions are observed for both $\bar{N}_{K^o_s}$ and $\bar{N}_\Lambda$ while in pp interactions at 205 GeV[4)] a linear dependence is observed for K^o_s but not for Λ.

The rapidity distributions in the π^--nucleon center-of-mass system are presented in Figs. 2a, b, c. Figure 2a indicates that γ production peaks in the central region and is approximately symmetric with respect to the forward and backward hemispheres. In the remainder of the paper, we restrict ourselves to γ's backward in the CMS. K^o_s production is reasonably flat from $y^* = 0$ to $y^* = -2$, beyond which it falls off, suggesting central production; whereas, Λ production is strongly damped near $y^* = 0$ and peaks at approximately $y^* = -2$. The $\bar{\Lambda}$'s (not shown) are also centrally produced. The

---

†Recently it has been observed[6)] that if one separates the diffractive and non-diffractive components in pp interactions at 205 GeV, there is considerably less correlation between $\bar{N}_\gamma$ and n_-.

same general features in $d\sigma/dy^*$ have been observed in $\pi^\pm p$ interactions at 100 GeV.[7,8)]

The function

$$F_1(x) = \frac{2}{\pi\sqrt{s}} \int E_{CM} \frac{d^2\sigma}{dx\,dp_T^2}\, dp_T^2$$

which gives the dependence of the invariant inclusive cross section on the scaling variable x, is plotted in Figs. 3a, b, c for γ, K^o_s, and Λ production respectively.† $F_1(x)$ shows a very sharp decrease away from $x = 0$ for γ production and may be well fit by $A\exp(Bx)$, with $A = 18.6 \pm 0.5$ and $B = 11.5 \pm 0.7$. K^o_s production also falls off away from $x = 0$, with an indication that it turns over near $x = 0.15$. In the case of Λ production, there is a rapid fall off near $x = 0$ and $x = 1$ and a broad peak at $x \approx 0.5$, which confirms that Λ's are produced mostly by target fragmentation.

The open circles shown in Fig. 3 are the inclusive cross sections obtained in pp interactions at 205 GeV[4)] scaled by $\sigma_{INEL}(\pi^-d)/\sigma_{INEL}(pp)$. The good agreement between the two sets of data is evidence for factorization in the backward hemisphere. Since the $F_1(x)$ distribution obtained in π^-p interactions at 205 GeV[3] also agrees well with the appropriately scaled pp data, and since the deuteron is a loosely-bound system, we expect our scaled $F_1(x)$ distribution to agree with that obtained in pp interactions.

In order to compare π^o production to $\pi^\pm$ production, we have used a sample of 809 measured events of all topologies to Monte Carlo the production of π^o's and their decay to $\gamma\gamma$. In the Monte Carlo, it was assumed that after

---

†$x = 2p_L/\sqrt{s}$ where p_L and E_{cm} are the momentum along the beam direction and the energy of the particle in the cm system defined for π-nucleon collisions assuming the nucleon to be at rest (i.e. neglecting the Fermi motion of the nucleons) in the lab.

the removal of obvious protons (identified by ionization) from the 809 events, the remaining tracks are π^+ or π^-, and that π^o production obeys the relation

$$\frac{d\sigma(\pi^o)}{dp_\mu} = \frac{1}{2}\left[\frac{d\sigma(\pi^+)}{dp_\mu} + \frac{d\sigma(\pi^-)}{dp_\mu}\right]^\dagger ,$$

where $p_\mu \cong p_L^*$ or p_T. The Monte Carlo prediction (smooth curve) and the measured $F_1(x)$ and $F_2(p_T^2)$ distributions (data points) are shown in Figs. 4a and 4b, respectively. The agreement between the measured data and the Monte Carlo prediction is seen to be good.

The dependence of the invariant inclusive neutral cross section on p_T^2 is given in Figs. 5a, b, c where we plot the function

$$F_2\ (p_T^2) = \frac{2}{\pi\sqrt{s}} \int_{-1}^{0} E_{cm}\ \frac{d^2\sigma}{dx dp_T^2}\ dx .$$

The expected exponential fall off with increasing p_T^2 is observed. The solid lines in Figs. 5a and b are fits to the function $A\exp(-Bp_T^2)$. Slopes are presented in Table 4 and compared with $\pi^- p$[3] and pp[4] interactions at 205 GeV. We note that the K_s^o and Λ dependence on p_T^2 are similar and agree well with the results from $\pi^- p$ and pp experiments.

The average values of p_T, p_T^2, $|p_L^*|$, $|p_L^{*2}|$ are presented in Table 5. We obtain the average values for π^o production by using

$$\left\langle p_T^2\right\rangle_{\pi^o} = 3\left\langle p_T^2\right\rangle_\gamma - 1/2\ m_\pi^2,\ \left\langle p_L^*\right\rangle_{\pi^o} = 2\left\langle p_L^*\right\rangle_\gamma,\ \left\langle p_L^{*2}\right\rangle_{\pi^o} = 3\left\langle p_L^{*2}\right\rangle_\gamma - 1/4\ m_\pi^2$$

(see Ref. 9). We use only γ's backward in the CMS and assume that they all originate from π^o decays and have symmetric distributions in the CMS.

---

†This relation was experimentally found to hold for $pp \to \gamma + x$ at 205 GeV (K. Jaeger et al., Ref. 4).

The average values agree well with those obtained in pp interactions at 205 GeV.[4]

The Λ polarization for $\pi^- d \to \Lambda + x$ has been calculated using $P = \frac{3}{\alpha} < \cos\theta >$ with $\alpha = 0.647$.† We obtain $P = 0.13 \pm 0.14$ which is consistent with no polarization. pp interactions at 205 GeV also observe no Λ polarization.[4]

4. DOUBLE SCATTERING EFFECTS

In Ref. 1 we have reported that double scattering occurs in approximately 14% of the total $\pi^- d$ interactions at 205 GeV. Similar results have been reported for $\pi^\pm d$ and pd reactions at several energies.[10] In this section, we investigate double scattering effects for interactions in which neutral particles are produced.

In order to study double scattering effects we separate our data into effective $\pi^- n$ interactions ("$\pi^- n$") and effective $\pi^- p$ interactions ("$\pi^- p$"). The "$\pi^- n$" category contains all events with odd-charged multiplicity plus the even multiplicities in which one of the tracks is an identifiable backward proton or a proton of momentum less than 280 MeV/c. The "$\pi^- p$" category contains all the remaining even-charged multiplicity events. The total cross sections for $n_{CH} \geq 3$ for "$\pi^- n$" and "$\pi^- p$" are given in Table 6 where we clearly observe an excess of "$\pi^- p$" events. The excess of neutral production in "$\pi^- p$" interactions occurs for all charge multiplicities as

---

†The normal to the production plane is given by $\hat{n} = \hat{p}_{\pi^-} \times \hat{\Lambda}$ where $\hat{p}_{\pi^-}$ and $\hat{\Lambda}$ are unit vectors defining the directions of the beam and Λ in the laboratory. The Λ decay angular distribution is given by $W(\cos\theta) = 1/2(1 + \alpha P\cos\theta)$, where $\cos\theta = \hat{n} \cdot \hat{p}$ and $\hat{p}$ is the momentum of the decay proton in the Λ rest frame.

can be seen in Table 6. As has been stressed in Ref. 1, the "$\pi^- p$" category contains contributions not only from true $\pi^- p$ interactions but also from $\pi^- n$ and $\pi^- p$ interactions in which there has been a second scatter on the spectator nucleon. If we assume that the inclusive neutral production cross section is equal for $\pi^- p$ and $\pi^- n$ interactions at 205 GeV, the excess of "$\pi^- p$" events, when summed over all n_{CH}, is a measure of the amount of double scattering present in deuterium. In this context, the ratio

$$f = \frac{\sigma(\text{"}\pi^- p\text{"}) - \sigma(\text{"}\pi^- n\text{"})}{\sigma(\text{"}\pi^- p\text{"}) + \sigma(\text{"}\pi^- n\text{"})}$$

gives the fraction of double scattering. Values of the ratio f for interactions involving neutral particles are given in Table 7. Within errors, the f values are consistent with the value 14% which we have reported in Ref. 1 for total $\pi^- d$ interactions.

Double scattering effects can be studied in more detail by looking at the dependence of f on y^* and p_T. In Fig. 6 we present f as a function of y^*. Since in this case we are comparing ratios, the corrections for losses cancel; thus, we extend the rapidity distributions to the forward hemisphere in the cases where there are sufficient data. The K_s^o and Λ distributions are within statistics flat and show no particular structure. However, for γ production the distribution of f shows a slight tendency to peak at large negative values of y^*. The statistical significance of this increase is not great; however, we note that most double scattering models would predict an excess of events at large negative y^*.[11] This is consistent with the trend we have observed in high multiplicity events.[12]

In Fig. 7 we present the dependence of f on p_T. In all cases, the distributions are consistent with a straight line of zero slope although

there is a marginal indication that γ production has a slight excess at approximately 250 MeV/c.

We conclude that we are observing a significant amount of double scattering in interactions in which neutral particles (γ, K_s^o, Λ) are produced. Assuming the equality of $\pi^- p$ and $\pi^- n$ cross sections, the amount of double scattering is consistent with the $\sim$ 14% double scattering observed for all events in $\pi^- d$ interactions at 205 GeV.[1]

5. $\pi^- n$ INCLUSIVE RESULTS

In this section we obtain results for $\pi^- n \to (\gamma, K_s^o, \Lambda) + x$ by correcting the effective "πn" interactions discussed in Section 4 for double scattering (1/2 of 14%) and Glauber shielding (4%). The procedures can be tested by applying the same corrections to the effective "$\pi^- p$" data and comparing the results to $\pi^- p$ interactions in hydrogen at the same energy (Ref. 3).

The comparison to hydrogen is given in Table 8 for the inclusive cross section for $n \geq 3$. Within errors both the $\pi^- n$ and $\pi^- p$ cross sections obtained for K_s^o and Λ production in this experiment agree with the results of π^- interactions in hydrogen at 205 GeV[4]. For γ production, the derived $\pi^- n$ cross section is lower by approximately 3 standard deviations than the π^--hydrogen cross section while the derived $\pi^- p$ cross section agrees within 1 standard deviation. The dependence of $\pi^- n$ and $\pi^- p$ cross sections (derived in this experiment) on charge multiplicity are displayed in Table 9.

The approximate agreement between $\pi^- p$ cross sections derived from $\pi^- d$ interactions with results from the direct $\pi^- p$ experiment suggests that $\pi^- n$ interactions may be measued in $\pi^- d$ experiments after suitable corrections for rescattering and screening effects have been applied. In the remainder of

the paper, we present the $\pi^- n$ results thus obtained and compare, whenever possible, with hydrogen results.

In Figs. 8a-c and 9a-c, we present the $F_1(x)$ and $d\sigma/dy^*$ distributions for $\pi^- n$ interactions derived from our data. Only the $F_1(x)$ distributions for K_s^o and Λ production at 205 GeV in π^- hydrogen are available for comparison. For both final states the shapes of the distributions from $\pi^- n$ interactions are very similar to those obtained from π^-- hydrogen interactions.

In Figs. 10 a-c we present the average number of γ, K, and Λ produced per inelastic $\pi^- n$ collision as a function of the number of negative particles produced (n_-). We plot in addition the result from the direct $\pi^- p$ experiment (Ref. 3) and note the close agreement. For $n_- \leq 8$ the behavior of $\bar{N}_\gamma$ is well parameterized by $\bar{N}_\gamma = \alpha + \beta n_-$ with $\alpha = 0.83 \pm 0.42$ and $\beta = 0.62 \pm 0.13$. For higher n_- the statustics are poorer and therefore the data are not used in the fit. We note that $\bar{N}_{K_s^o}$ may be increasing with increasing n_- (although it is also consistent with being flat) and fits well the relation $\bar{N}_{K_s^o} = \alpha + \beta n_-$ for all n_- with $\alpha = 0.051 \pm 0.010$ and $\beta = 0.011 \pm 0.003$. A fit to $\bar{N}_\Lambda$ gives $\alpha = 0.014 \pm 0.009$ and $\beta = 0.008 \pm 0.003$ (the data are consistent with no dependence on n_-).

In summary, we suggest that $\pi^- p$ and $\pi^- n$ interactions can be separated by taking into account a 14% probability of rescattering in the deuteron. The $\pi^- n$ inclusive distributions are found, within statistics, to be the same as those obtained for $\pi^- p$ interactions in hydrogen.

We would like to thank the staffs of the 30-inch bubble chamber and neutrino laboratories at FNAL and our scanning and measuring staffs for their assistance. We are indebted to S. Ellis, M. Szeptycka, and A. Wroblewski for critical comments and suggestions. Two of us, H. Rudnicka, and A. Zieminski, would like to thank the University of Washington for its generous hospitality

REFERENCES:

1. K. Dziunikowska et al., Phys. Letters 61B (1976) 316.
2. J. H. Klema et al., Acta Physica Polonica B7 (1976) 497.
3. D. Ljung et al., "$\pi^- p$ at 205 GeV/c: Multiplicities of Charged and Neutral Particles; Production of Neutral Particles". FERMILAB-PUB-76/92-EXP - to be published in Phys. Rev.
4. K. Jaeger et al., Phys. Rev. D11 (1975) 45.
5. J. Whitmore, Phys. Reports 10C (1974).
6. J. Whitmore, Phys. Reports 27C (1976).
7. E. L. Berger et al., "Production of K_s^o, Λ, and γ in 100 GeV/c $\pi^- p$ Interactions", CERN/D.Ph.II/PHYS 74-27, submitted to the XVIIth International Conference on High-Energy Physics, London (1974).
8. M. Alston-Garnjost et al., Phys. Rev. Letters 35 (1975) 142.
9. G. I. Kopylov, Phys. Lett. 41B (1972) 371.
10. S. Dado et al., Phys. Letters 60B, (1976) 397 and J. E. A. Lys et al. To be published in Phys. Rev. ($\pi^+ d$ and pd at 100 GeV); Y. Eisenberg et al., Phys. Letters 60B (1976) 305 (pd and $\pi^+ d$ at 195 GeV); T. Dombeck et al., ANL-HEP-PR-76-62 - to be published in Nuc. Phys. (pd at 200 GeV).
11. K. Gottfried, Phys. Rev. Letters 32 (1974) 957; Y. Afek et al., "Rapidity Distributions in Hadron-Nucleus Collisions". Preprint Technion PH-76-48 - to be published; J. H. Weis, Acta Physica Polonica B7 (1976) 851.
12. Davis-Krakow-Seattle-Warsaw Collaboration. "Double Scattering Effects in High-multiplicity $\pi^- d$ Interactions". Presented at the XVIII International Conference on High Energy Physics, Tbilisi, July 15-21, 1976 - to be published.

13. T. M. Knasel, DESY Reports Nos. 70/2 and 70/3, 1970 (unpublished).
14. A. S. Carroll et al., Phys. Letters 61B (1976) 304.

TABLE CAPTIONS:

TABLE 1: Cross sections for neutral particle production in $\pi^- d$ collisions.

TABLE 2: Topological cross sections for neutral particle production for $x < 0$ in $\pi^- d$ collisions.

TABLE 3: Average number of neutral particles per inelastic $\pi^- d$ collision.

TABLE 4: Slope parameters from fit of $A\exp(-Bp_T^2)$ to $F_2(p_T^2)$ for $\pi^- d$, $\pi^- p$ and pp interactions at 205 GeV.

TABLE 5: Average values of transverse and longitudinal momenta.

TABLE 6: Effective "$\pi^- n$" and "$\pi^- p$" cross sections for $n_{CH} \geq 3$, where B and F indicate backward ($x < 0$) and forward ($x > 0$) in CMS, respectively.

TABLE 7: Topological cross sections for "$\pi^- n$" and "$\pi^- p$" for $x < 0$.

TABLE 8: Total cross sections for $\pi^- p$ and $\pi^- n$ corrected for double scattering and Glauber shielding.

TABLE 9: Topological cross sections for $\pi^- n$ and $\pi^- p$ interactions corrected for double scattering and Glauber shielding.

TABLE 1

Neutral Particle		Number of Fitted Neutrals	Average Weights $\langle w \rangle$ †	Correction Factor ††	Cross Section (mb)	No. Produced per Inelastic Collision ($n_{CH} \geq 3$) This Experiment	$\pi^- p$ 205 GeV (Ref. 3)	pp 205 GeV (Ref. 4)
γ	Backward	516	70.5	1.23	120 ± 10	3.39 ± 0.30	4.27 ± 0.32	3.55 ± 0.25
γ	Forward	491	53.0	1.51	106 ± 15	2.99 ± 0.42		3.55 ± 0.25
K_s^o	Backward	379	2.32	1.31	3.07 ± 0.30	0.087 ± 0.009	0.096 ± 0.013	0.096 ± 0.007
Λ	Backward	205	2.56	1.29	1.77 ± 0.20	0.050 ± 0.006	0.057 ± 0.011	0.054 ± 0.005
$\bar{\Lambda}$	Backward	22	3.01	1.30	0.41 ± 0.15	0.012 ± 0.005	0.017 ± 0.007	0.013 ± 0.004
π^o	†††				113 ± 9	3.19 ± 0.25		3.34 ± 0.24

† Based on detection efficiencies. γ conversion probabilities were determined from the data of Ref. 13.

†† Corrects for scanning, measuring, and fitting losses.

††† Assuming that all γ's originate from π^o decay.

TABLE 2

No. of Charged Particles Observed	CROSS SECTIONS (mb) $\pi^- d \to \gamma + X$	$\pi^- d \to K_s^o + X$	$\pi^- d \to \Lambda + X$
3	1.45 ± 0.54	0.078 ± 0.028	0.039 ± 0.018
4	5.66 ± 1.33	0.213 ± 0.042	0.156 ± 0.038
5	4.02 ± 1.04	0.109 ± 0.030	0.046 ± 0.021
6	14.40 ± 2.23	0.349 ± 0.055	0.202 ± 0.040
7	5.10 ± 1.13	0.204 ± 0.042	0.135 ± 0.037
8	20.42 ± 2.65	0.458 ± 0.061	0.252 ± 0.047
9	7.62 ± 1.66	0.137 ± 0.035	0.132 ± 0.039
10	18.32 ± 2.55	0.472 ± 0.063	0.242 ± 0.047
11	5.76 ± 1.24	0.068 ± 0.026	0.060 ± 0.023
12	13.85 ± 2.17	0.382 ± 0.059	0.203 ± 0.041
13	2.21 ± 1.02	0.094 ± 0.028	0.030 ± 0.015
14	7.58 ± 1.42	0.221 ± 0.042	0.108 ± 0.031
15	2.46 ± 0.96	0.061 ± 0.022	0.060 ± 0.023
16	5.09 ± 1.07	0.101 ± 0.030	0.048 ± 0.023
17	0.68 ± 0.37	$0.002^{+0.005}_{-0.001}$	0.020 ± 0.011
18	4.19 ± 1.10	0.076 ± 0.024	$0.007^{+0.017}_{-0.003}$
19	$0.35^{+0.60}_{-0.19}$	$0.014^{+0.025}_{-0.008}$	$0.008^{+0.019}_{-0.003}$
20	$0.33^{+0.60}_{-0.19}$	$0.018^{+0.043}_{-0.007}$	$0.015^{+0.034}_{-0.006}$
21	$0.11^{+0.26}_{-0.04}$	$0.006^{+0.014}_{-0.002}$	$0.000^{+0.009}_{-0.000}$
22	$0.11^{+0.26}_{-0.04}$		$0.013^{+0.031}_{-0.005}$
23	$0.21^{+0.50}_{-0.08}$		
24	$0.13^{+0.31}_{-0.05}$		

TABLE 3

No. of Negative Particles Produced	Average Number of Neutrals per Inelastic Collision $\pi^- d \to \gamma^B + X$	$\pi^- d \to K_s^{o(B)} + X$	$\pi^- d \to \Lambda^B + X$
1	1.23 ± 0.25	0.050 ± 0.009	0.034 ± 0.007
2	2.76 ± 0.37	0.068 ± 0.009	0.037 ± 0.007
3	3.48 ± 0.40	0.090 ± 0.010	0.052 ± 0.008
4	4.27 ± 0.51	0.100 ± 0.012	0.062 ± 0.010
5	4.44 ± 0.58	0.102 ± 0.015	0.060 ± 0.011
6	3.72 ± 0.68	0.120 ± 0.019	0.052 ± 0.013
7	5.55 ± 1.08	0.119 ± 0.028	0.079 ± 0.024
8	7.49 ± 2.02	0.120 ± 0.040	$0.040^{+0.071}_{-0.022}$
9	$2.29^{+2.29}_{-0.718}$	$0.106^{+0.186}_{-0.062}$	$0.073^{+0.128}_{-0.013}$
10	$1.82^{+3.21}_{-1.08}$	$0.050^{+0.12}_{-0.02}$	$0.109^{+0.260}_{-0.050}$
11	$8.27^{+14.66}_{-5.14}$		

TABLE 4

Particle	Slope Parameter B $(GeV/c)^2$		
	$\pi^- d$	$\pi^- p$ (3)	pp (4)
K^o_s	3.61 ± 0.33	3.97 ± 0.50	4.6 ± 0.8
Λ	3.57 ± 0.21	3.18 ± 0.14	2.8 ± 0.8

TABLE 5

	$< p_T >$, (GeV/c)	$< p_T^2 >$, $(GeV/c)^2$	$< p_L^* >$, (GeV/c)	$< p_L^{*2} >$, $(GeV/c)^2$
γ	0.175 ± 0.008 (0.199 ± 0.008)*	0.065 ± 0.005 (0.078 ± 0.001)	0.311 ± 0.021 (0.317 ± 0.021)	0.288 ± 0.043 (0.345 ± 0.061)
π^o		0.186 ± 0.015 (0.244 ± 0.003	0.622 ± 0.042 (0.634 ± 0.042)	0.852 ± 0.129 (1.03 ± 0.18)
K^o_s	0.457 ± 0.014 (0.412 ± 0.014)	0.262 ± 0.017 0.234 ± 0.019	1.17 ± 0.05 (1.07 ± 0.05)	2.43 ± 0.24 (1.98 ± 0.23)
Λ	0.504 ± 0.023 (0.504 ± 0.026)	0.346 ± 0.031 (0.345 ± 0.033)	3.75 ± 0.16 (3.84 ± 0.19)	18.6 ± 1.3 (19.6 ± 1.5)

*The average values for pp experiment at 205 GeV/c[4] are given in brackets.

TABLE 6

No. of Charged Particles (n_{CH})*	σ "$\pi^- n$" (mb)			σ "$\pi^- p$" (mb)		
	γ^B	$K_s^{o\,B}$	Λ^B	γ^B	$K_s^{o\,B}$	Λ^B
3	3.1 ± 1.0	0.134 ± 0.035	0.039 ± 0.018			
4				4.1 ± 1.1	0.157 ± 0.036	0.156 ± 0.038
5	6.8 ± 1.4	0.212 ± 0.043	0.076 ± 0.025			
6				11.6 ± 2.1	0.246 ± 0.046	0.171 ± 0.037
7	7.8 ± 1.4	0.312 ± 0.051	0.155 ± 0.039			
8				17.7 ± 2.5	0.350 ± 0.053	0.231 ± 0.046
9	10.4 ± 1.9	0.218 ± 0.044	0.176 ± 0.044			
10				15.5 ± 2.4	0.391 ± 0.058	0.198 ± 0.042
11	8.0 ± 1.5	0.190 ± 0.043	0.111 ± 0.031			
12				11.6 ± 2.0	0.261 ± 0.048	0.152 ± 0.036
13	3.4 ± 1.2	0.144 ± 0.035	0.036 ± 0.016			
14				6.4 ± 1.4	0.171 ± 0.036	0.101 ± 0.030
15	4.6 ± 1.2	0.072 ± 0.025	0.077 ± 0.029			
16				2.9 ± 0.8	0.089 ± 0.028	0.031 ± 0.015
17	1.2 ± 0.5	0.024 ± 0.013	0.020 ± 0.011			
18				3.7 ± 1.0	0.054 ± 0.021	$0.007^{+0.017}_{-0.003}$
19	$0.35^{+0.60}_{-0.19}$	$0.014^{+0.025}_{-0.008}$	$0.008^{+0.019}_{-0.003}$			
20				$0.34^{+0.60}_{-0.19}$	$0.018^{+0.043}_{-0.007}$	$0.014^{+0.034}_{-0.006}$
21	$0.11^{+0.26}_{-0.04}$	$0.006^{+0.014}_{-0.002}$	$0.000^{+0.009}_{-0.000}$			
22				$0.11^{+0.26}_{-0.04}$		$0.013^{+0.031}_{0.005}$
23	$0.34^{+0.60}_{-0.19}$					

* Identified spectators are not included in the prong count.

TABLE 7

PARTICLE	σ("πn"), mb ($n_{CH} \geq 3$)	σ("πp"), mb ($n_{CH} \geq 3$)	$f = \frac{\sigma(\text{"}\pi p\text{"}) - \sigma(\text{"}\pi n\text{"})}{\sigma(\text{"}\pi p\text{"}) + \sigma(\text{"}\pi n\text{"})}$
γ(B)	46.0 ± 6.0	74.0 ± 8.0	0.23 ± 0.06
γ(F)	43.7 ± 10.0	62.3 ± 12.0	0.18 ± 0.12
π^o	44.8 ± 6.0	68.2 ± 7.0	0.21 ± 0.06
K_s^o(B)	1.33 ± 0.20	1.74 ± 0.22	0.13 ± 0.07
Λ(B)	0.70 ± 0.13	1.07 ± 0.15	0.21 ± 0.09

TABLE 8

PARTICLE	$\sigma(\pi^- n)$	$\sigma(\pi^- p)$	$\sigma(\pi^- p)^{(3)}$
γ(B)	56.6 ± 6.	68.3 ± 8.0	82.5 ± 5.9
γ(F)	53.2 ± 10.	57.1 ± 12.0	
π^o	57.1 ± 6.	65.1 ± 7.0	
K_s(B)	1.60 ± .20	1.59 ± 0.22	1.85 ± 0.24
Λ(B)	0.85 ± 0.13	0.99 ± 0.15	1.11 ± 0.22

TABLE 9

n_{CHGD}	$\sigma(\pi^- n)$ (mb)			$\sigma(\pi^- p)$ (mb)		
	γ^B	K_S^B	Λ^B	γ^B	K_S^B	Λ^B
3	3.69 ± 1.0	0.16 ± 0.04	0.06 ± 0.02			
4				3.69 ± 1.1	0.14 ± .04	0.15 ± 0.04
5	8.41 ± 1.5	0.25 ± 0.05	0.10 ± 0.03			
6				10.72 ± 2.1	0.22 ± .05	0.16 ± 0.04
7	9.97 ± 1.5	0.37 ± 0.05	0.19 ± 0.04			
8				16.55 ± 2.6	0.31 ± .06	0.21 ± 0.05
9	12.7 ± 2.0	0.27 ± 0.05	0.21 ± 0.05			
10				14.24 ± 2.5	0.36 ± .06	0.18 ± 0.04
11	9.75 ± 1.6	0.24 ± 0.03	0.13 ± 0.03			
12				10.64 ± 2.1	0.24 ± .05	0.14 ± 0.04
13	4.25 ± 1.2	0.17 ± 0.04	0.05 ± 0.02			
14				5.94 ± 1.5	0.16 ± .04	0.10 ± 0.03
15	5.34 ± 1.2	0.09 ± 0.03	0.09 ± 0.03			
16				2.48 ± 0.83	0.08 ± .03	0.024 ± .016
17	1.55 ± .50	0.03 ± 0.01	0.023 ± 0.011			
18				3.49 ± 1.0	0.06 ± .02	$0.0053^{+.017}_{-.003}$
19	$0.42^{+0.62}_{-0.20}$	0.02 ± 0.01	$0.01^{+0.19}_{-.003}$			
20				$0.30^{+0.62}_{-0.20}$	0.02 ± .02	$0.013^{+.034}_{-.006}$
21	$0.14^{+0.27}_{-0.04}$		$.001^{+.009}_{-.001}$			
22				$0.09^{+0.27}_{-0.04}$		$0.013^{+.031}_{-.005}$
23	$0.35^{+0.62}_{-0.20}$					

FIGURE CAPTIONS

FIG. 1 : Dependence of the average number of neutrals on the number of negative particles produced (n_-). The curves are fits to $\alpha + \beta n_-$ from $n_- = 1$ to $n_- = 8$.

a) Backward γ's.

b) All γ's.

c) Backward K^o_s's.

d) Backward Λ's.

FIG. 2 : Rapidity distributions in the pi-nucleon cm system.

a) $\pi^- d \to \gamma + x$ b) $\pi^- d \to K^o_s + x$ c) $\pi^- d \to \Lambda + x$.

FIG. 3 : The inclusive distribution $F_1(x)$ for neutrals produced in $\pi^- d$ interactions (this experiment) compared to results from pp interactions (Ref. 4).

a) (•) $\pi^- d \to \gamma + X$ and (o) $pp \to \gamma + X$;

b) (•) $\pi^- d \to K^o_s + X$ and (o) $pp \to K^o_s + X$;

c) (•) $\pi^- d \to \Lambda + X$ and (o) $pp \to \Lambda + X$.

FIG. 4 : a) The inclusive distribution $F_1(x)$ for $\pi^- d \to \gamma + x$;

b) The inclusive distribution $F_2(p_T^2)$ for $\pi^- d \to \gamma + x$.

The smooth curve is obtained from the Monte Carlo calculation described in the text.

FIG. 5 : The inclusive distribution $F_2(p_T^2)$ for:

a) $\pi^- d \to \gamma + X$; b) $\pi^- d \to K^o_s + X$; c) $\pi^- d \to \Lambda + X$.

The curves are fits to $A\exp(-Bp_T^2)$; (see Table 4).

FIG. 6 : Dependence of the fraction of double scattering (f) on y^* for:

a) $\pi^- d \to \gamma + x$; b) $\pi^- d \to K^o_s + x$; c) $\pi^- d \to \Lambda + x$.

FIG. 7 : Dependence of the fraction of double scattering (f) on p_T for:

a) $\pi^- d \to \gamma + x$; b) $\pi^- d \to K^o_s + x$; c) $\pi^- d \to \Lambda + x$.

FIG. 8 : $F_1(x)$ for neutrals produced in $\pi^- n$ interactions (this experiment) compared to results from $\pi^- p$ interactions (Ref. 3).

a) (•) $\pi^- n \to \gamma + x$;

b) (•) $\pi^- n \to K^o_s + x$ and

(o) $\pi^- p \to K^o_s + x$.

c) (•) $\pi^- n \to \Lambda + x$ and

(o) $\pi^- p \to \Lambda + x$.

FIG. 9 : $d\sigma/dy^*$ for a) $\pi^- n \to \gamma + x$; b) $\pi^- n \to K^o_s + x$; c) $\pi^- n \to \Lambda + x$.

FIG. 10 : The dependence of the average number of neutrals on the number of negative particles produced in $\pi^- n$ interactions (this experiment) is compared to results in $\pi^- p$ interactions (Ref. 3).

a) (•) $\pi^- n \to \gamma + x$ and (x) $\pi^- p \to \gamma + x$;

b) (•) $\pi^- n \to K^o_s + x$ and (x) $\pi^- p \to K^o_s + x$;

c) (•) $\pi^- n \to \Lambda + x$ and (x) $\pi^- p \to \Lambda + x$.

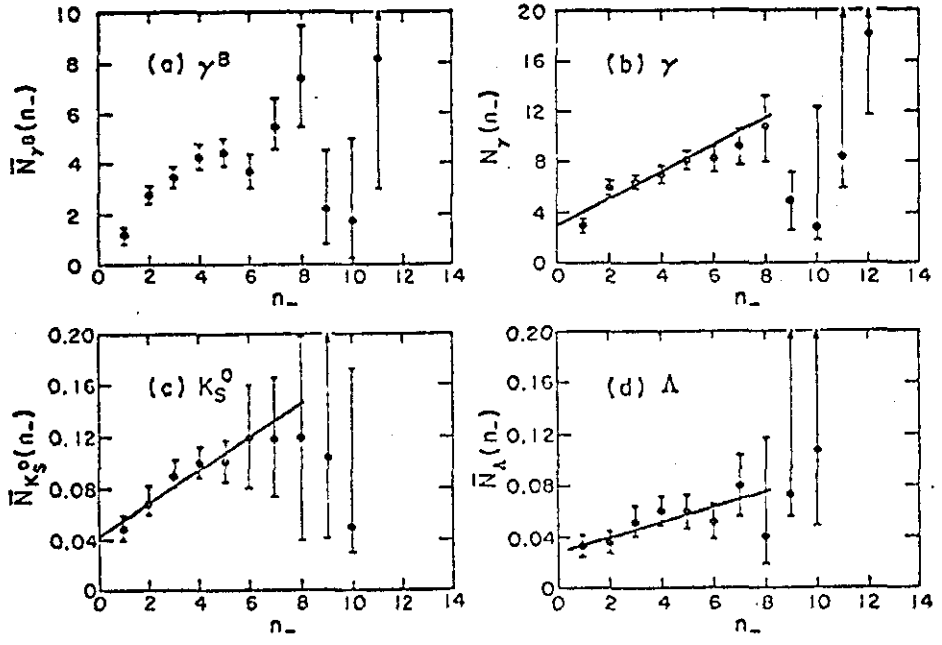
(a) γ^B
(b) γ
(c) K_S^0
(d) Λ
$\bar{N}_{\gamma^B}(n_-)$
$N_\gamma(n_-)$
$\bar{N}_{K_S^0}(n_-)$
$\bar{N}_\Lambda(n_-)$
n_-

FIG. 1

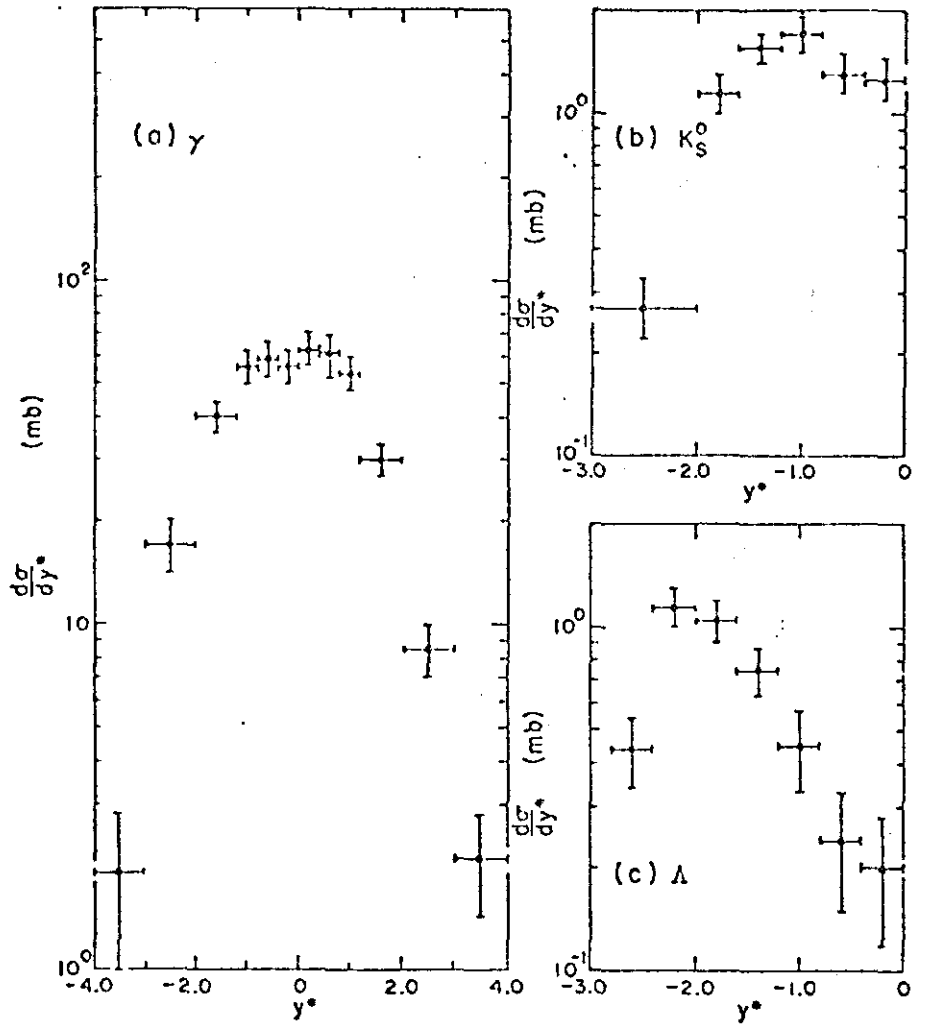
(a) γ
(b) K_S^0
(c) Λ
$\frac{d\sigma}{dy^*}$ (mb)
y^*

FIG. 2

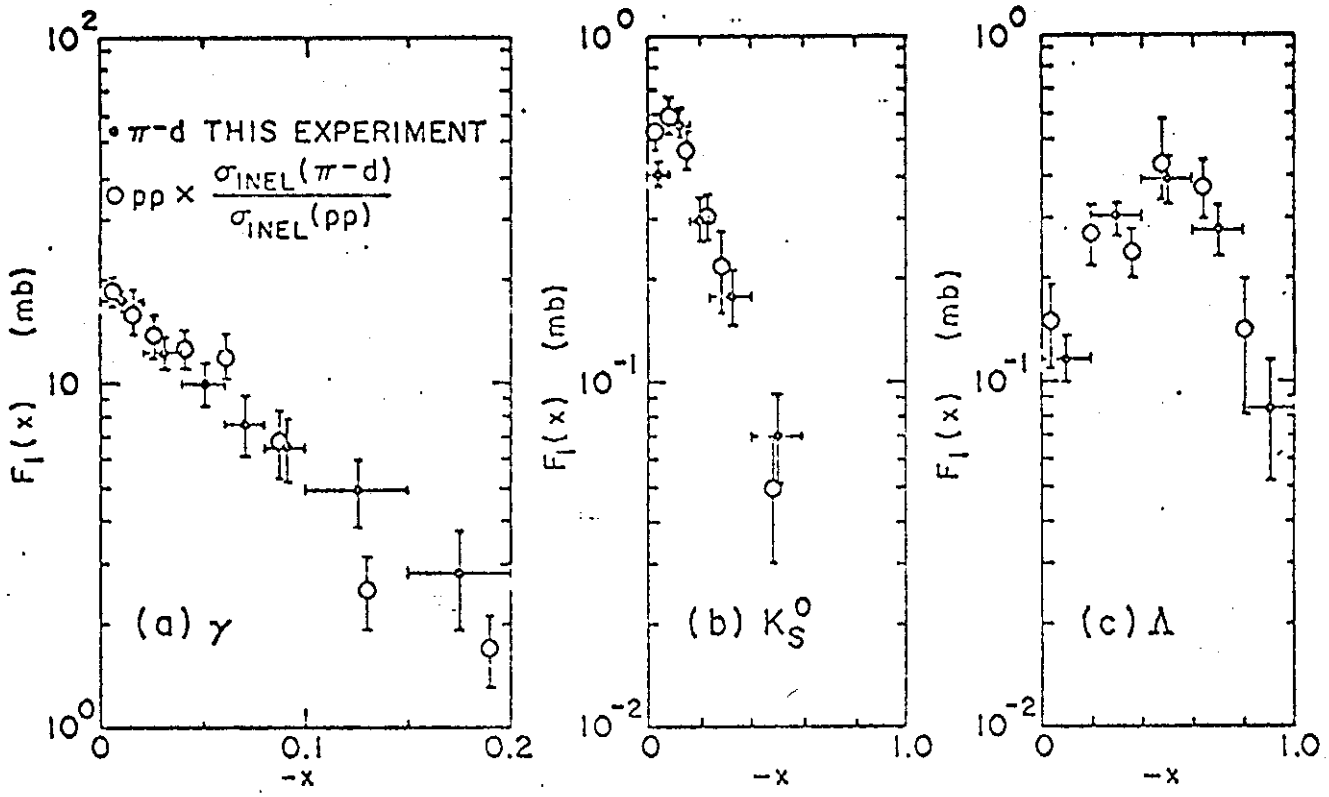
• π⁻d THIS EXPERIMENT
○ pp × σINEL(π⁻d) / σINEL(pp)
(a) γ
(b) K⁰S
(c) Λ
F1(x) (mb)
−x

FIG. 3

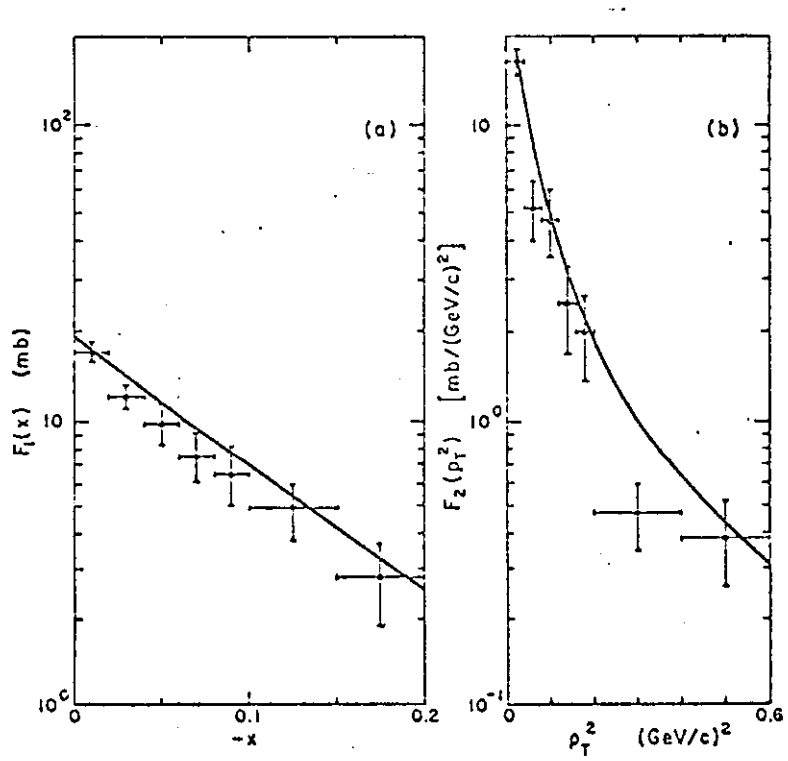
(a)
(b)
F1(x) (mb)
F2(pT²) [mb/(GeV/c)²]
−x
pT² (GeV/c)²

FIG. 4

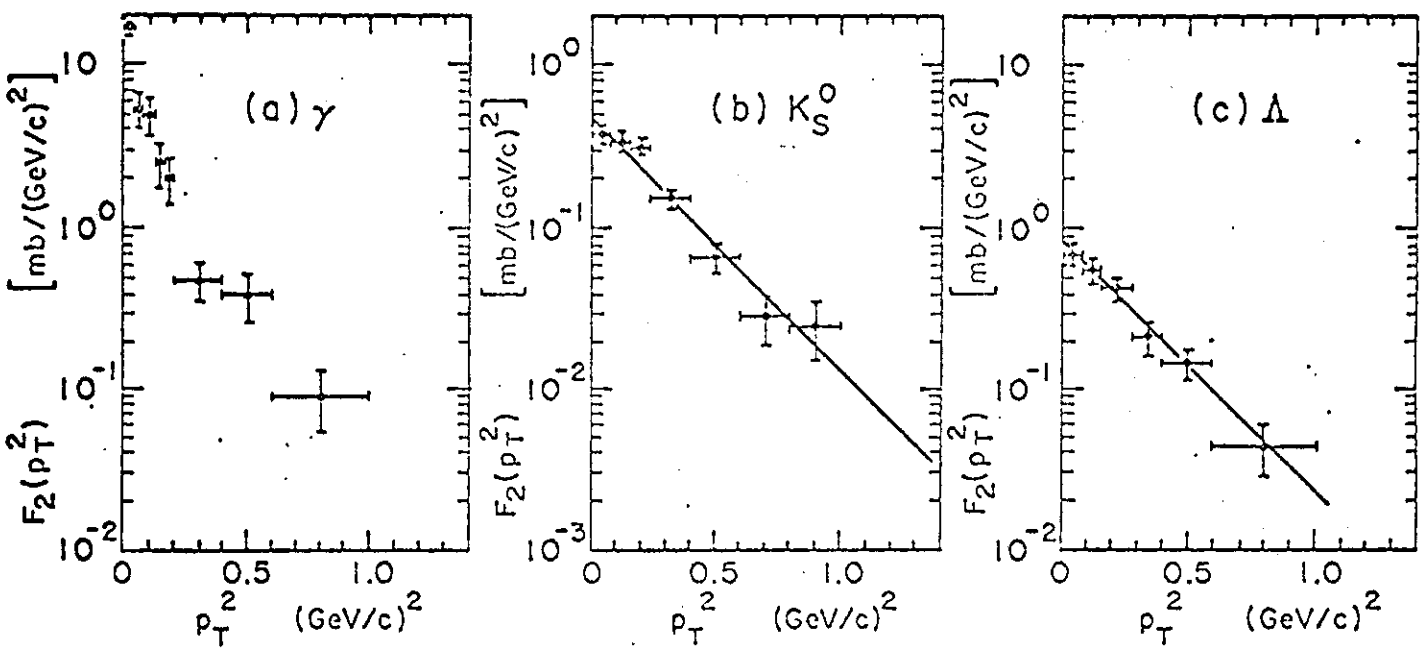

FIG. 5

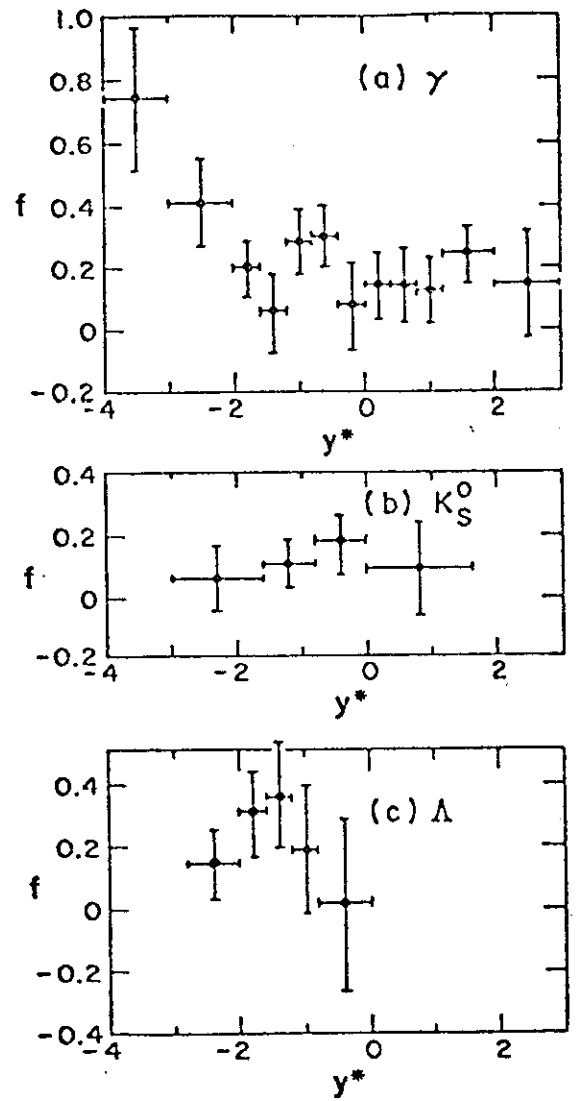

FIG. 6

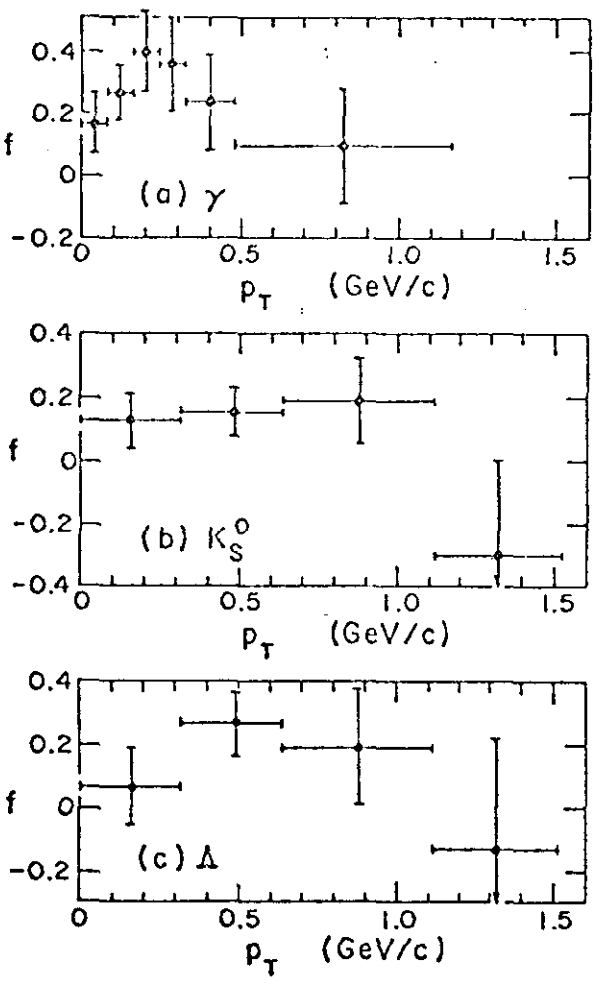

FIG. 7

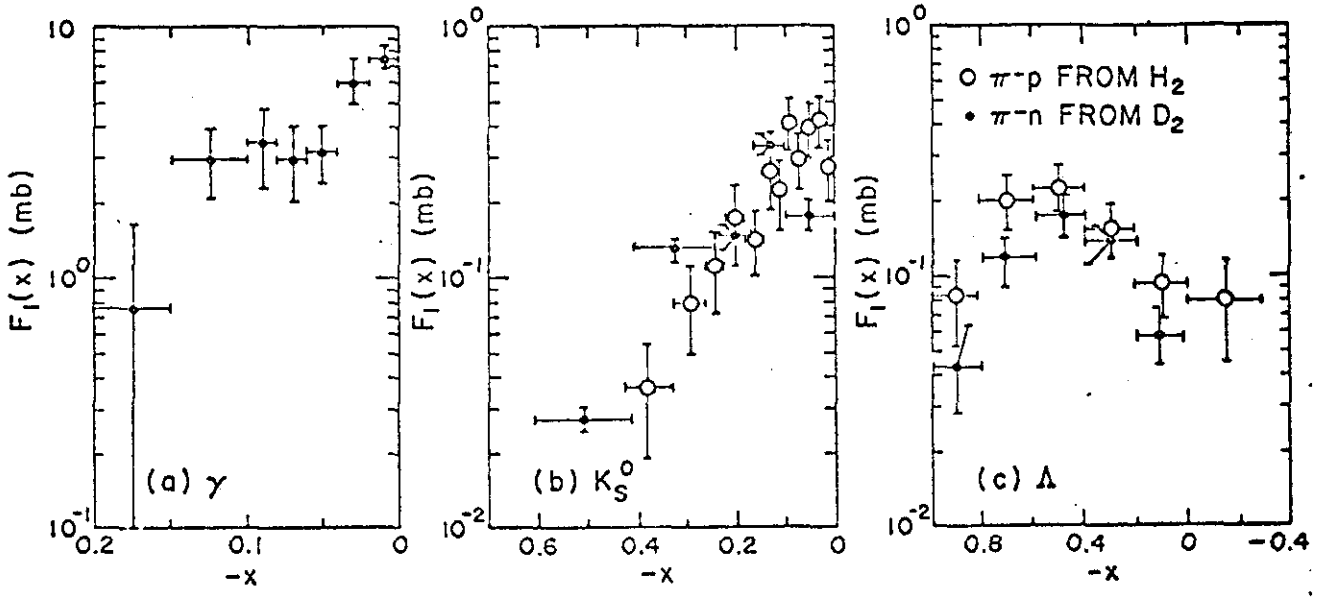

FIG. 8

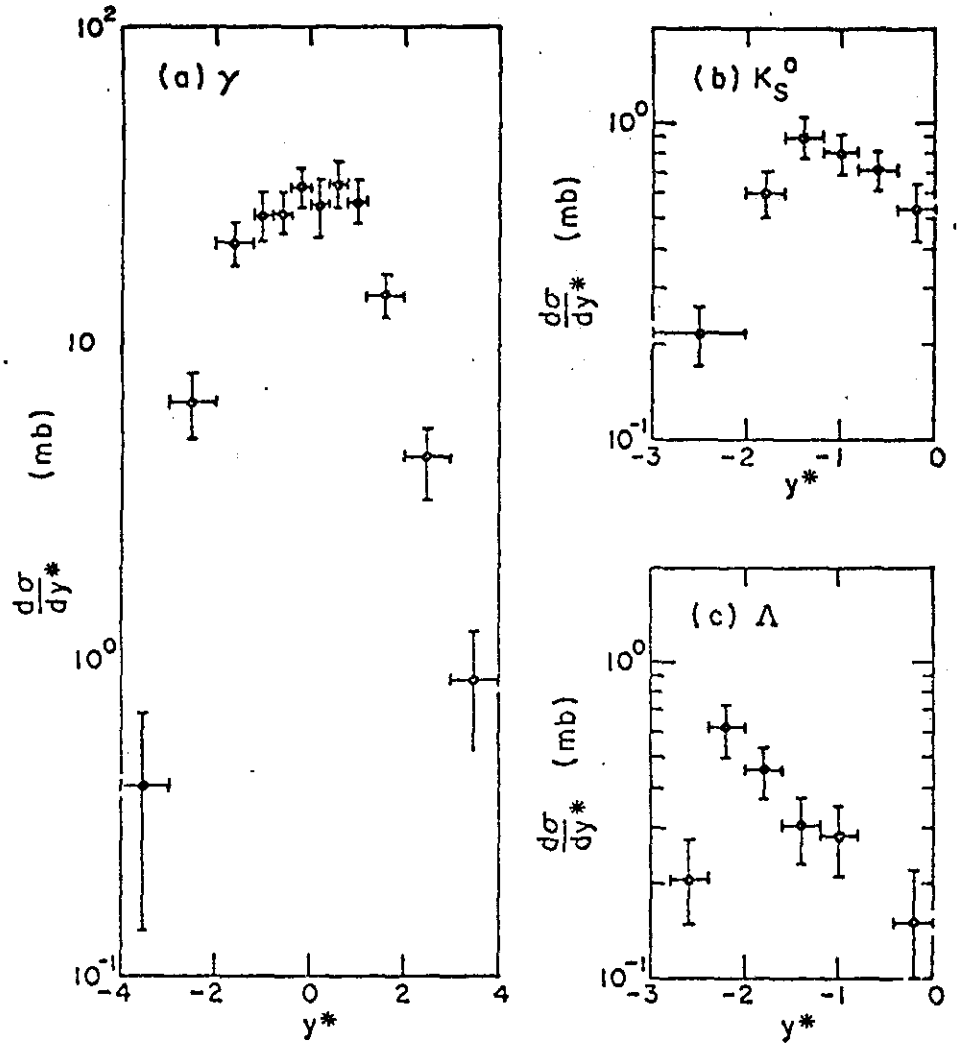
(a) γ
(b) K_S^0
(c) Λ
$\frac{d\sigma}{dy^*}$ (mb)
y*

FIG. 9

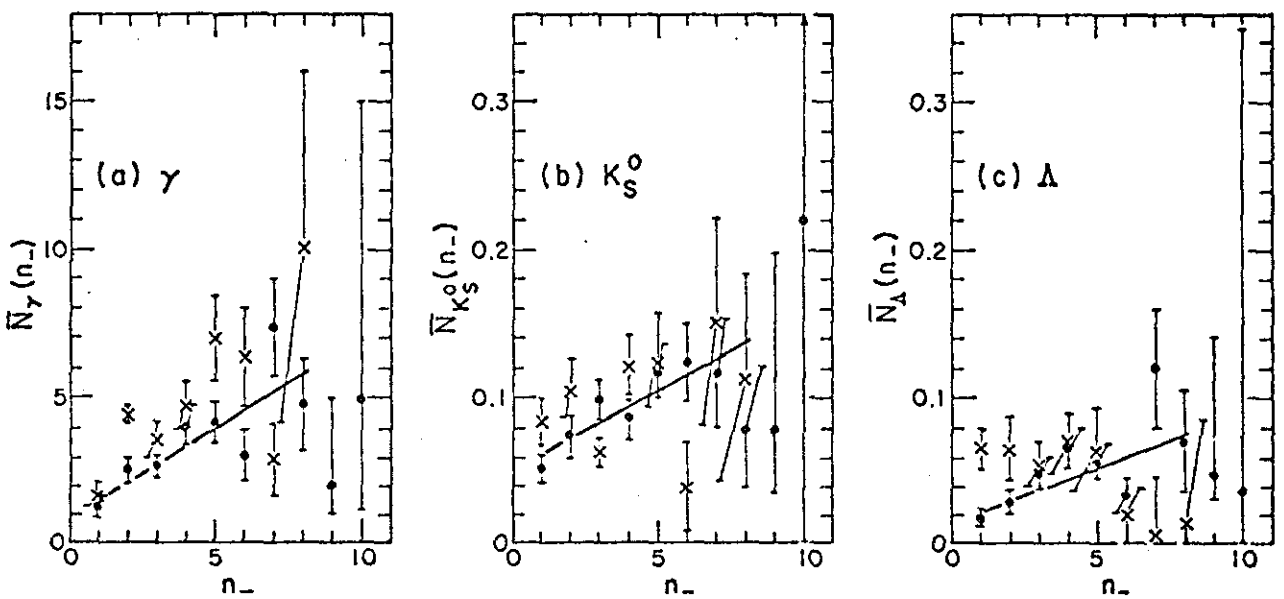
(a) γ
(b) K_S^0
(c) Λ
$\bar{N}_\gamma(n_-)$
$\bar{N}_{K_S^0}(n_-)$
$\bar{N}_\Lambda(n_-)$
n_-

FIG. 10